PHOTONIC SENSORS / Vol. 7, No. 3, 2017: 246–252

Distributed Fiber Optic Interferometric Geophone System Based on Draw Tower Gratings

Ruquan XU*, Huiyong GUO, and Lei LIANG

National Engineering Laboratory for Fiber Optic Sensing Technology, Wuhan University of Technology, Wuhan, 430070, China

*Corresponding author: Ruquan XU E-mail: xuruquan@whut.edu.cn

Abstract: A distributed fiber optic interferometric geophone array based on draw tower grating (DTG) array is proposed. The DTG geophone array is made by the DTG array fabricated based on a near-contact exposure through a phase mask during the fiber drawing process. A distributed sensing system with 96 identical DTGs in an equal separation of 20 m and an unbalanced Michelson interferometer for vibration measurement has been experimentally validated compared with a moving-coil geophone. The experimental results indicate that the sensing system can linearly demodulate the phase shift. Compared with the moving coil geophone, the fiber optic sensing system based on DTG has higher signal-to-noise ratio at low frequency.

Keywords: Fiber optic sensing; vibrating sensing; draw tower grating; interferometric geophone

Citation: Ruquan XU, Huiyong GUO, and Lei LIANG, "Distributed Fiber Optic Interferometric Geophone System Based on Draw Tower Gratings," *Photonic Sensors*, 2017, 7(3): 246–252.

1. Introduction

Seismic exploration technology has been widely employed for the exploration of oil and other mineral resources, detection of geological hazards, hydrographic surveys, rail vibrations, debris flow, and engineering quality inspection [1–3]. Seismic exploration and monitoring for oil and gas reservoirs is a peculiar application that requires a large number of geophones deployed outdoors over large areas to detect backscattered waves from artificial sources. A storing and processing system collects the data from all the geophones to get an image of the sub-surface. The existed cabling system to connect sensors is known to cause inefficiencies, electromagnetic interference, and weight cost, as well as insufficient flexibility in survey design [4]. Therefore, the development of a new type geophone with higher multiplexing capacity is one of the keys to improve the detection capabilities of seismic surveys. Compared with traditional geophones, the fiber Bragg grating (FBG) geophone owns many advantages, such as immunity to electromagnetic interference, remote sensing, and multiplexing capacity, which makes FBG particularly suitable for multipoint sensing [5]. The FBG accelerometer can receive the acceleration with the help of wavelength demodulation schemes such as scanning Fabry-Perot filters [6], edge filter methods [5, 7], or interferometric techniques [8]. An eight-element fiber laser geophone array system was presented in [9]. However, these fiber optic sensors multiplexing capacity on a single fiber only reaches 20–30. In this paper, we propose a distributed fiber optic interferometric geophone system based on identical DTGs. The sensor system is constructed by an identical low

Received: 25 February 2017 / Revised: 20 April 2017

DOI: 10.1007/s13320-017-0408-2
Article type: Regular

reflectivity DTG array fabricated based on a near-contact exposure through a phase mask during the fiber drawing process. The adjacent DTGs construct a Fabry-Perot (F-P) vibration sensor, which is sensitive to vibration. For the ultralow reflectivity of the DTGs and no fusion points between DTGs, this system has larger capacity than traditional fiber optic geophone system.

2. DTG array fabrication

The fabrication technique presented here is based on a near-contact exposure through a phase mask during the fiber drawing process. The draw tower grating fabrication setup is shown in Fig. 1. For increasing the single pulse photosensitivity, we used a highly photosensitive Ge/B co-doped preform. The fiber preform was heated in a furnace up to a temperature of more than 2 000 ℃ and was then drawn with a velocity of approximately 12 m/min into a bare fiber with a final diameter of 125 μm. Before the fiber was coated, Bragg gratings were inscribed using a line-narrowed ArF excimer laser (OptoSystems, CL5300), with a beam size of 4×12 (mm), pulse width of 10 ns, maximum pulse energy of 40 mJ, and maximum laser repetition rate of 300 Hz based on phase mask method.

The UV (ultraviolet) laser writing setup was placed on the draw tower to synchronize with the grating inscription to reduce the vibration between the bare fiber and the laser beam. The laser beam (pulse energy of 25 mJ) was normally incident on the 1 550 nm phase mask and diffracted entirely. A slit was attached to the mask and transferred only 5 mm of the exposing beam to the bare fiber. The DTG was formed by the interference between the +1 and –1 diffracted orders of the phase mask. Thus, the refractive index of the fiber core was periodically changed. The interference fringes were determined by the structure of the phase mask and not influenced by light source coherence, which ensured the good wavelength consistency of the DTGs.

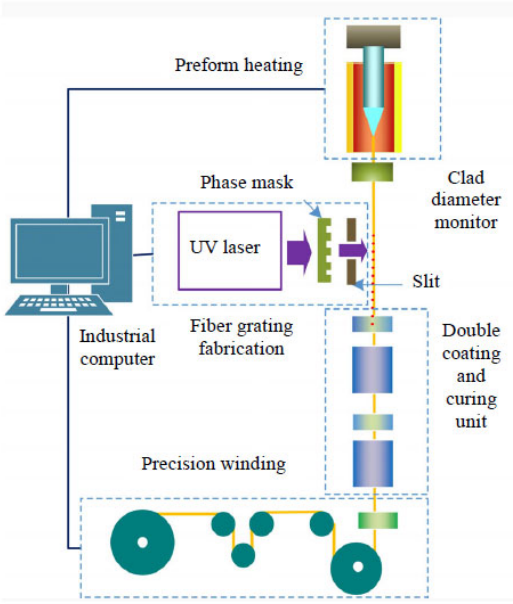

Fig. 1 Diagram for DTGs fabrication experimental setup.

The control computer fixed the laser pulse repetition at 0.01 Hz to synchronize the grating inscription, and the distance between adjacent DTGs was 20 m. Directly after the grating inscription, the DTG fiber was coated, and the coating was cured under UV light.

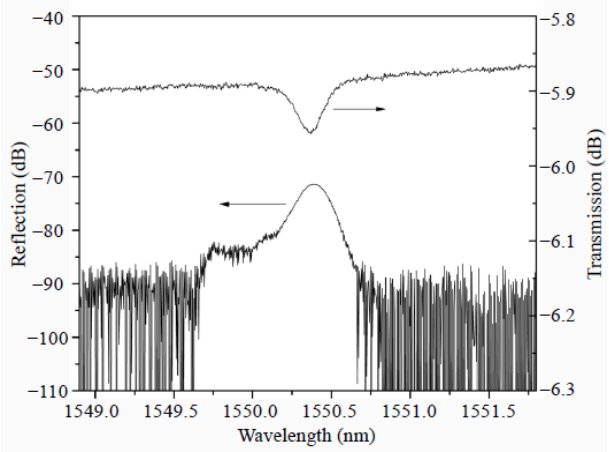

Fig. 2 Reflection and transmission spectra of the DTG array.

For measuring the reflection spectrum of DTGs, a standard setup with a superluminescent diode optical source (spectral range from 1 510 nm to 1 570 nm), an optical circulator, and an optical spectrum analyzer (OSA, Yokogawa, AQ6370C) was used. The reflection and transmission spectra of the DTGs are shown in Fig. 2. The central wavelength of the DTGs is 1 550.4 nm, the spectrum

width of the DTGs is 0.2 nm (–3 dB). The results indicate that on-line writing DTGs using the phase mask method have a central wavelength with good uniformity. The DTG array contains 96 DTGs, and the distance between adjacent DTGs is 20 m. The DTG average reflectivity is 0.015%.

3. Experimental setup and operation principle

The experimental setup for the measurement of the ground vibration signals is shown in Fig. 3. The sensor system is constructed with 48 DTG F-P interferometers (containing two adjacent identical DTGs) and an unbalanced Michelson interferometer. To get distributed information along a DTG fiber, the reflection signals from each DTG F-P interferometer are detected. Narrow linewidth coherent light pulses are used as probe pulses with a wavelength close to the central wavelength of the DTG array. The reflection signals are coupled into an unbalanced Michelson interferometer comprised of a 2×2 and a 3×3 fiber coupler. The difference in the fiber length between the two arms of the Michelson interferometer is equal to two times of the difference in fiber length between two adjacent DTGs. The reflected signals of the first pulse from DTG1 and the reflected signals of the second pulse from DTG2 are coupled into an unbalanced Michelson interferometer, and then interference occurs at the 3×3 coupler. Therefore, with a probe pulse injected into the DTGs, the reflected waves at the two arms of the unbalanced Michelson interferometer can be expressed respectively as

$$E_a(t)=\frac{\sqrt{2}}{2}\sum_{i=1}^{N}E_0\sqrt{(1-R)^{2(i-1)}R}\times \exp\{\mathrm{j}2\pi f(t-\tau_i)\}\mathrm{rect}\left(\frac{t-\tau_i}{W}\right) \quad (1)$$

$$E_b(t)=\frac{\sqrt{2}}{2}\sum_{i=1}^{N}E_0\sqrt{(1-R)^{2(i-1)}R}\times \exp\{\mathrm{j}2\pi f(t-\tau_i-\tau_0)\}\mathrm{rect}\left(\frac{t-\tau_i-\tau_0}{W}\right) \quad (2)$$

where R is the reflectivity of the DTG$_i$ ($i=1, 2, \cdots, N$), N is the total number of the DTGs, L_0 is the fiber distance of the adjacent two DTGs, f is the frequency of the probe pulse, and τ_0 is the round trip time of the probe pulse between two adjacent DTGs. $\tau_0=2n_{\mathrm{eff}}L_0/c$, τ_i is the time delay of DTG$_i$. For avoiding interfering with each other, the width of the probe pulse $W<2n_{\mathrm{eff}}L_0/c$. n_{eff} is the effective refractive index, and c is the vacuum light speed.

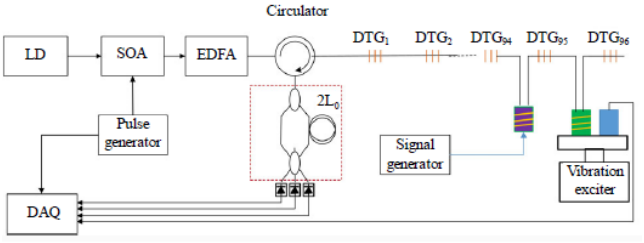

Fig. 3 Diagram of experimental setup.

Therefore, $E_a(t)$ interferes with $E_b(t)$ at the 3×3 coupler, and the three interference outputs of the symmetric 3×3 coupler in the Michelson interferometer can be expressed as

$$I_k(t)=\sum_{i=1}^{N-1}\left[D_i+E_i\cos\left(\varphi_{i,i+1}-(k-2)\frac{2\pi}{3}\right)\right]\times \mathrm{rect}\left(\frac{t-\tau_{i+1}}{W}\right),\ k=1,2,3 \quad (3)$$

with

$$D_i=\frac{1}{3}E_0^2R(1-R)^{2(i-1)} \quad (4)$$

$$E_i=\frac{1}{3}E_0^2R(1-R)^{2(i-1)} \quad (5)$$

where $\varphi_{i,i+1}$ is the phase shift between DTG$_i$ and DTG$_{i+1}$. D_i is the direct component determined by the optical power and gain in the detection electronics, and E_i is the AC component determined by the 2×2 coupler splitting ratio and the polarization states of the two arms of the Michelson interferometer.

If the Michelson interferometer is stable, the phase shift $\varphi_{i,i+1}$ between DTG$_i$ and DTG$_{i+1}$ is given as

$$\varphi_{i,i+1}=2\pi fn_{\mathrm{eff}}(L_{i+1}-L_i)/c-\varphi_0 \quad (6)$$

where L_i and L_{i+1} are the distances from the input to DTG$_i$ and DTG$_{i+1}$, respectively; φ_0 is the phase

difference of the Michelson interferometer. The three interference outputs of the symmetric 3×3 coupler in the Michelson interferometer can be expressed as [10]

$$V_{\text{out}}(t)=\sum_{i=1}^{N-1}S_i\varphi_{i,i+1}\text{rect}\left(\frac{t-\tau_{i+1}}{W}\right) \tag{7}$$

where S_i is dependent on the electronics amplifier and is set as $\sqrt{3}$ in the software program. Therefore, $V_{\text{out}}(t)$ at τ_2, τ_3, $\cdots$, τ_N can be expressed as $V_{i,\text{out}}=S_i\cdot\varphi_{i,i+1}$, and the phase shift is as follows:

$$\varphi_{i,i+1}=\frac{1}{S_i}V_{i,\text{out}}=\frac{V_{i,\text{out}}}{\sqrt{3}}. \tag{8}$$

So we can obtain the phase shift by measuring the amplitude of the demodulated signal, $V_{i,\text{out}}$. Thus, for a symmetric 3×3 coupler, the demodulated result is free from the optical power and the reflectivity of the DTGs.

The intrinsic multiple reflections crosstalk phenomenon in the inline DTG-FFP sensor system is a serious problem that limits the multiplexing number of sensors, which comes from the light reflected two more times by DTGs other than the target DTG but reaching the 3×3 coupler at the same time with the real signal. For the DTG array with identical low reflectivity, only the first-order crosstalk (signals undergoing three reflections) needs to be considered. Then the worst crosstalk for the DTG sensor system with n DTGs is given as follows [11]:

$$C_{\text{DTG}_i,\text{DTG}_{i+1}}=20\lg\left(\frac{iR}{1-R}\right). \tag{9}$$

The worst crosstalk is dependent on the reflectivity of the DTGs and the multiplexing number of DTGs. Figure 4 shows the worst crosstalk in the DTG sensor systems with different multiplexing numbers of DTGs when the reflectivities are 1%, 0.1%, 0.01%, and 0.001%, which shows the worst crosstalk increases as an increase in the multiplexing number of DTGs with fixed reflectivity.

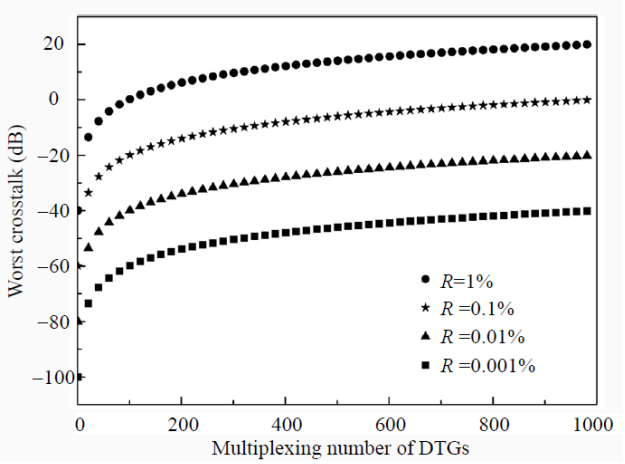

Fig. 4 Crosstalk verses the multiplexing number of DTG at different reflectivities.

4. Experiment and results

An 1 550 nm coherent laser with 5 mW (Santec, TLS510) was pulsed by an optical semiconductor amplifier (SOA, INPHNEX 1502) to create 100 ns optical pulses with 100 kHz repetition rate. The SOA driving current was modulated by signal generator (RIGOL, DG1022) with pulsed signals. The optical pulses were amplified by an erbium-doped fiber amplifier (EDFA) and filtered by a narrow band optical filter and then coupled into DTG sensor array by a circulator. The reflections of the DTGs injected into an unbalanced Michelson interferometer consisting of a 2×2 coupler and a 3×3 coupler. The interference signals converted from the symmetric 3×3 coupler were coupled into three photodetectors, and then the signals were acquired by DAQ (NI, PXI-5122) and processed by a software program.

4.1 Optical phase demodulation

In order to further demonstrate the multiplexing system phase shift demodulation performance, the fiber between DTG_{94} and DTG_{95} was coiled on a commercial piezoelectric ceramic transducer (PZT), which was driven by a signal generator (RIGOL, DG1022). The PZT could change the phase shift linearly on the fiber between DTG_{94} and DTG_{95}. The PZT was driven by 10 Hz and 200 Hz sine signals, respectively. Figures 5(a) and 5(b) demonstrate the time domain figures of the phase

shift of 10 Hz and 200 Hz sine signals, which shows the sensing system can demodulate the phase shift in real time. Figure 6 shows the frequency spectrum of phase shift of 10 Hz and 200 Hz sine signals provided in Fig. 5. The system dynamic scope reaches 27 dB at 10 Hz and 40 dB at 200 Hz, respectively. Therefore, the technique presented in this paper provides a practical method of interrogating as many as 96 sensors with a large dynamic range. Further gains may be realized by decreasing the reflection of the DTGs, as can be seen from Fig. 4. When the driving signal frequency was fixed at 10 Hz, we obtained the linearity of demodulated phase shift by tuning the amplitude of the driving signal. Figure 7 shows that the linearity of demodulated phase shift is 0.99. The result indicates that our fiber optic interferometric geophone system based on identical DTGs can properly demodulate the instantaneous time and frequency domain signals with good linearity.

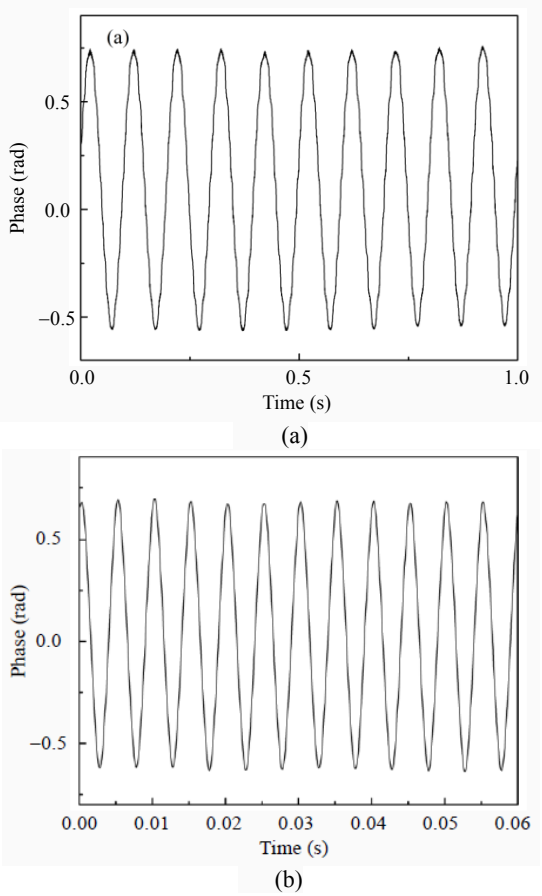

Fig. 5 Time domain signal of (a) 10 Hz and (b) 200 Hz.

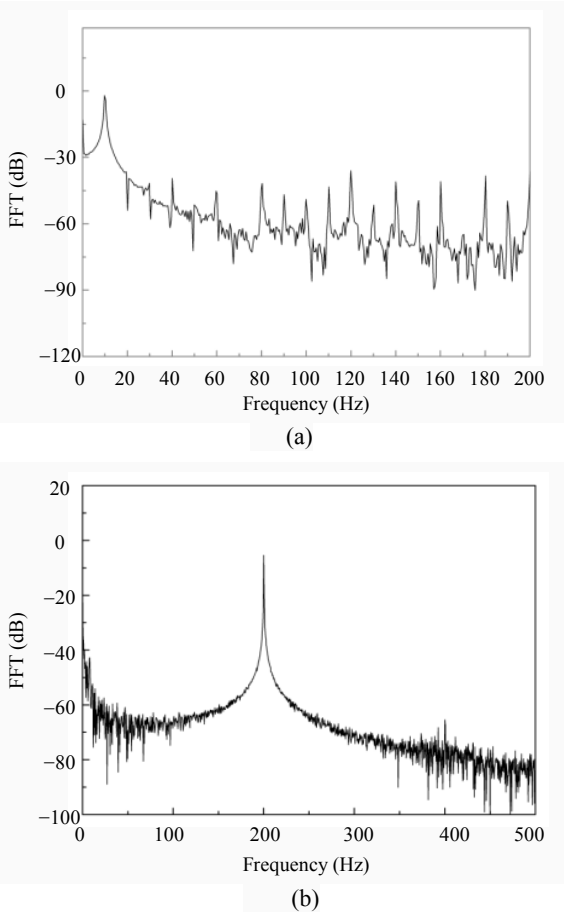

Fig. 6 Frequency domain signal of (a) 10 Hz and (b) 200 Hz.

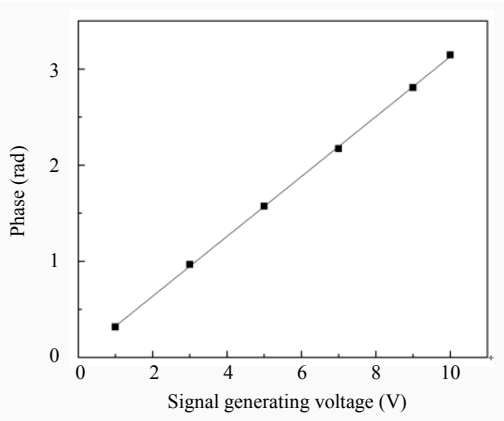

Fig. 7 Demodulated amplitude with different signal generating voltages at 10 Hz.

4.2 Vibration experiment

For validating the vibration demodulation performance, the fiber between DTG_{95} and DTG_{96} was coiled on a compliant cylinder to detect the vibration signals [12]. In order to compare with the conventional moving-coil geophone, we fixed the fiber sensor and a moving-coil geophone

(SGO-15HT) on the same vibrator (DH40500). The output signal of the SGO-15HT was amplified and filtered by an amplifier (SR810). When the vibrator outputs 80 Hz vibration signal to simulate seismic wave, the response signals from 0 s to 0.1 s demodulated by the fiber optic sensor and SGO-15HT are shown in Figs. 8(a) and 8(b), respectively. Figure 8 indicates that the demodulated 80 Hz signal by the fiber sensor system fits well with the signal detected by the conventional moving-coil geophone, which has a good sinusoidal shape. Figures 9(a) and 9(b) show the frequency spectrum of the Figs. 8(a) and 8(b), respectively. Compared with the moving-coil geophones, the signal demodulated by the fiber sensor system has higher signal-to-noise ratio at low frequency, but it contains more harmonic peaks, which is probably caused by the 3×3 coupler with asymmetry splitting ratio.

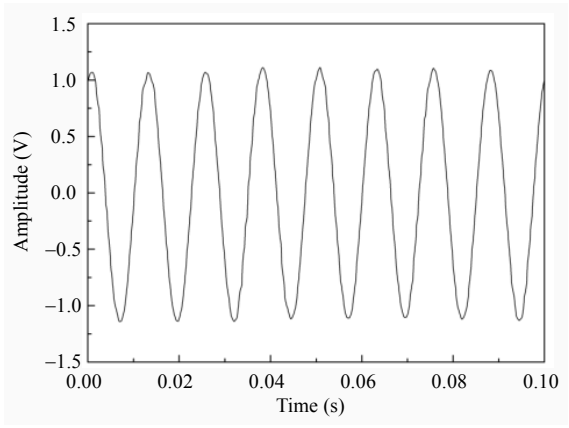

Fig. 8 Demodulated vibration signals by (a) fiber sensor and (b) SGO-15HT.

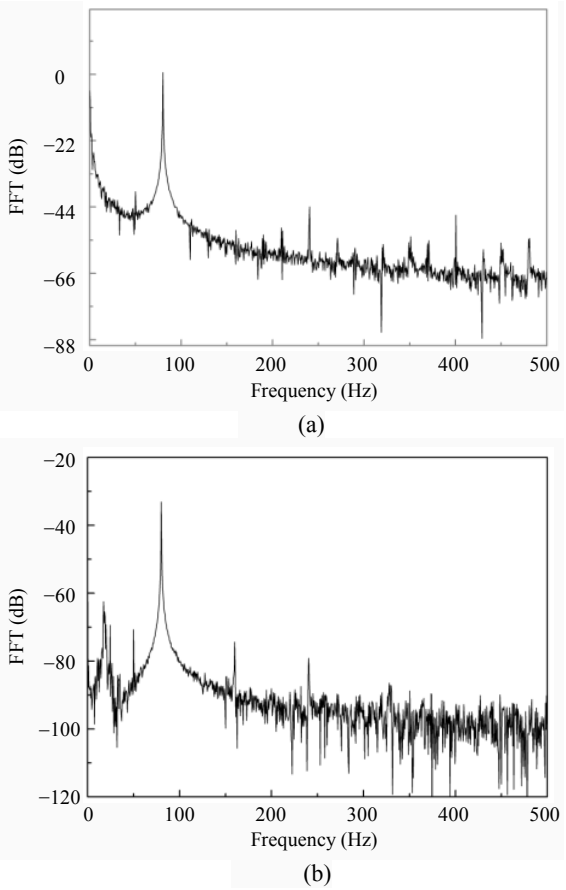

Fig. 9 Frequency responses of the demodulated vibration signals by (a) fiber sensor and (b) SGO-15HT.

5. Conclusions

A fiber optic interferometric multiplexing vibration sensing system based on DTG array is proposed and experimentally demonstrated in the paper. A DTG array with 96 DTGs was on line fabricated on the draw tower with 20 m distance between adjacent two DTGs. Phase modulation experimental results indicate that the sensing system phase demodulation dynamic scope reaches 27 dB at 10 Hz and 40 dB at 200 Hz, and the linearity of phase demodulation is 0.99 at 10 Hz when the DTGs multiplexing number reaches 96. Vibration experimental results show that the fiber optic sensing system based DTGs has larger multiplexing capacity and higher signal-to-noise ratio at low frequency than the moving coil geophone. The next step of the work is to optimize the sensor package to enhance the sensitivity and reduce the volume of the sensors.

Acknowledgment

This work was partly supported by the Major Program of the National Natural Science Foundation of China (Grant No. 61290311), the Fundamental Research Funds for the Central Universities (Grant No. 2015III056), and Key Consulting Project of Chinese Academy of Engineering (Grant No. 2016-XZ-13).

References

[1] G. Tao, X. L. Zhang, X. R. Liu, S. H. Chen, and T. Y. Liu, "A new type of fiber Bragg grating based seismic geophone," *Applied Geophysics*, 2009, 6(1): 84–92.

[2] I. Crespo-Chacon, J. L. Garcia-de-la-Oliva, and E. Santiago-Recuerda, "On the use of geophones in the low-frequency regime to study rail vibrations," *Procedia Engineering*, 2016, 143: 782–794.

[3] T. C. Liang and Y. L. Lin, "A fiber-optic sensor for the ground vibration detection," *Optics Communications*, 2013, 306(18): 190–197.

[4] S. Savazzi, U. Spagnolini, L. Goratti, D. Molteni, M. Latva-aho, and M. Nicoli, "Ultra-wide band sensor networks in oil and gas explorations," *IEEE Communications Magazine*, 2013, 51(4): 150–160.

[5] J. Y. Wang, B. X. Hu, W. Li, G. D. Song, L. Jiang, and T. Y. Liu, "Design and application of fiber Bragg grating (FBG) geophone for higher sensitivity and wider frequency range," *Measurement*, 2016, 79: 228–235.

[6] Z. G. Wang, W. T. Zhang, J. Han, W. Z. Huang, and F. Li, "Diaphragm-based fiber optic Fabry-Perot accelerometer with high consistency," *Journal of Lightwave Technology*, 2014, 32(24): 4208–4213.

[7] Q. Zhang, T. Zhu, J. D. Zhang, and K. S. Chiang, "Micro-fiber-based FBG sensor for simultaneous measurement of vibration and temperature," *IEEE Photonics Technology Letters*, 2013, 25(18): 1751–1753.

[8] A. D. Kersey, T. A. Berkoff, and W. W. Morey, "High resolution fiber grating based strain sensor with interferometric wavelength-shift detection," *Electronics Letters*, 1992, 28(3): 236–238.

[9] Z. H. Sun, X. H. Liu, F. X. Zhang, S. J. Li, X. L. Zhang, C. Wang, *et al*., "High sensitivity fiber laser geophone array and field test analysis," *Measurement*, 2016, 79: 216–221.

[10] F. F. Chen, Y. Jiang, and L. Jiang, "3×3 coupler based interferometric magnetic field sensor using a TbDyFe rod," *Applied Optics*, 2015, 54(8): 2085–2090.

[11] H. Z. Lin, L. N. Ma, Z. L. Hu, Q. Yao, and Y. M. Hu, "Multiple reflections induced crosstalk in inline TDM fiber Fabry-Perot sensor system utilizing phase generated carrier scheme," *Journal of Lightwave Technology*, 2013, 31(16): 2651–2658.

[12] Y. S. Zhang, X. G. Qiao, Q. P. Liu, D. K. Yu, H. Gao, M. Shao, *et al*., "Study on a fiber Bragg grating accelerometer based on compliant cylinder," *Optical Fiber Technology*, 2015, 26: 229–233.